Numerical Analysis of Current Attachment at Thermionic Cathode for Gas Tungsten Arc at Atmospheric Pressure†

YAMAMOTO Kentaro*, TASHIRO Shinichi and TANAKA Manabu*****

Abstract

In a gas tungsten arc at atmospheric pressure, electrons are emitted from a thermionic cathode of the tungsten electrode, of which the work function would be reduced by generally adding an emitter material such as thorium oxide (ThO_2), lanthanum oxide (La_2O_3), and so on. However, there is still a lack of practical understanding of the physical behavior in the electrode region. For example, current attachment at a thermionic cathode is not yet clear. The present paper presents a methodology for predicting the current attachment at a thermionic cathode for the gas tungsten arc at atmospheric pressure in argon. It is suggested that the current attachment at thermionic cathode is dependent on work function, melting point and the Richardson constant of emitter materials.

KEY WORDS: (Numerical simulation), (Gas tungsten arc), (Cathode)

1. Introduction

In gas tungsten arc at atmospheric pressure, electrons are emitted from a thermionic cathode of the tungsten electrode, of which the work function would be reduced by generally adding an emitter material such as thorium oxide (ThO_2), lanthanum oxide (La_2O_3), and so on [1)]. However, there is still a lack of practical understanding of the physical behavior in the electrode region. For example, current attachment at thermionic cathode is not yet clear. The emitter materials such as ThO_2, La_2O_3, etc would not only affect work function of the cathode but also current attachment at the cathode. The current attachment at the cathode affects the plasma state of the arc column due to change in the cathode jet induced by the Lorentz force at the cathode region [1, 2)]. It is well known that arc flames are dependent on the kinds of emitter materials which are added to the tungsten electrode. Welders, for example, suggest that a W-ThO_2 electrode produces a hard arc flame but a W-La_2O_3 electrode produces a soft arc one [3)]. The present paper presents a methodology for predicting the current attachment at a thermionic cathode for gas tungsten arc at atmospheric pressure in argon. We use a numerical model of a gas tungsten arc where the arc and its electrodes are treated as a unified system.

2. A unified model

The tungsten cathode, arc plasma and anode are described relative to a cylindrical coordinate, assuming rotational symmetry around the arc axis. The calculation domain is shown in **Fig. 1**. The flow is assumed to be laminar, and the arc plasma is assumed to be in local thermodynamic equilibrium (LTE). The diameter of the tungsten cathode is 3.2 mm with a 60 degrees conical tip. The anode is assumed to be water-cooled copper and its diameter is 50 mm with 10 mm in thickness.

The mass continuity equation is

$$\frac{1}{r}\frac{\partial}{\partial r}(r\rho v_r)+\frac{\partial}{\partial r}(\rho v_z)=0 \tag{1}$$

the radial momentum conservation equation is

$$\frac{1}{r}\frac{\partial}{\partial r}(r\rho v_r^2)+\frac{\partial}{\partial z}(\rho v_z v_r)=-\frac{\partial P}{\partial r}-j_z B_\theta + \frac{1}{r}\frac{\partial}{\partial r}(2r\eta\frac{\partial v_r}{\partial r})+\frac{\partial}{\partial z}(\eta\frac{\partial v_r}{\partial z}+\eta\frac{\partial v_z}{\partial r})-2\eta\frac{v_r}{r^2} \tag{2}$$

† Received on July 10, 2009
* Graduate school student
** Assistant Professor
*** Professor

Transactions of JWRI is published by Joining and Welding Research Institute, Osaka University, Ibaraki, Osaka 567-0047, Japan

the axial momentum conservation equation is

$$\frac{1}{r}\frac{\partial}{\partial r}(r\rho v_r v_z)+\frac{\partial}{\partial z}(\rho v_z^2)=-\frac{\partial P}{\partial z}+j_r B_\theta + \frac{\partial}{\partial z}(2\eta\frac{\partial v_z}{\partial z})+\frac{1}{r}\frac{\partial}{\partial r}(r\eta\frac{\partial v_r}{\partial z}+r\eta\frac{\partial v_z}{\partial r}) \quad (3)$$

the energy conservation equation is

$$\frac{1}{r}\frac{\partial}{\partial r}(r\rho v_r h)+\frac{\partial}{\partial z}(\rho v_z h)=\frac{1}{r}\frac{\partial}{\partial r}(\frac{r\kappa}{c_p}\frac{\partial h}{\partial r})+\frac{\partial}{\partial z}(\frac{\kappa}{c_p}\frac{\partial h}{\partial z}) + j_r E_r + j_z E_z - R \quad (4)$$

the current continuity equation is

$$\frac{1}{r}\frac{\partial}{\partial r}(rj_r)+\frac{\partial}{\partial z}(j_z)=0 \quad (5)$$

and the Ohm's law (6) is

$$j_r=-\sigma E_r ; j_z=-\sigma E_z \quad (6)$$

and Maxwell's equation is

$$\frac{1}{r}\frac{\partial}{\partial r}(rB_\theta)=\mu_0 j_z \quad . \quad (7)$$

where t is time, h is enthalpy, P is pressure, v_r and v_z are the radial and axial velocities, j_r and j_z are the radial and axial components of the current density, g is the acceleration due to gravity, κ is the thermal conductivity, c_p is the specific heat, ρ is the density, η is the viscosity, U is the radiation emission coefficient, σ is the electrical conductivity, B_θ is the azimuthal magnetic field, μ_0 is the permeability of free space, E_r and E_z are respectively the radial and axial components of the electric field defined by $E_r = -\partial V/\partial r$ and $E_z = -\partial V/\partial z$, where V is electric potential. Calculations at points on both electrode surfaces would need to include the special process occurring at the surfaces. Thus, additional energy flux terms need to be included in equation (4) at each electrode surface for thermionic heating and cooling from the electrons, ion heating, and radiation cooling. The additional energy flux for the cathode H_K and for the anode H_A are

$$\text{Cathode } H_K = -\varepsilon\alpha T^4 - |j_e|\,\varphi_K + |j_i|V_i \quad (8)$$

and

$$\text{Anode } H_A = -\varepsilon\alpha T^4 + |j_e|\,\varphi_A \quad (9)$$

respectively. Here ε is the surface emissivity, α is the Stefan-Boltzmann constant, φ_K is the work function of the tungsten cathode, φ_A is the work function of the anode, V_i is the ionization potential of helium, j_e is the electron current density, and j_i is the ion current density. We calculate the electron saturation current density at the cathode surface by thermionic emission of electrons j_R from the Richardson-Dushman equation. The ion current density j_i is then assumed to be $|j| < |j_R|$ if $|j|$ is greater than $|j_R|$; where $|j| = |j_e| + |j_i|$ is the total current density at the cathode surface obtained from equation. The detailed boundary conditions and numerical method are given in our previous paper [4]. Within both electrodes, we set $v_r = v_z = 0$. The temperatures at boundaries CD, DE, EF, and FA in Fig. 1 are taken to be the same room temperature, namely, 300 K. The electric potential is set to zero at the base of the anode, CD, in Fig.1. In order to avoid the problem that the equilibrium electrical conductivity is effectively zero in the plasma close to the electrodes owing to the low plasma temperature, we employ an LTE-diffusion approximation [5]. The differential equations (1) to (7) are solved iteratively by the SIMPLEC numerical procedure [6] for the whole region of the arc welding process.

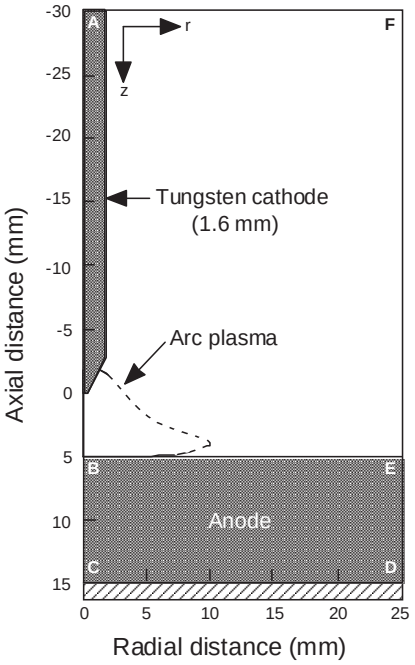

Fig. 1 Schematic illustration of simulation domain.

3. Treatment of current attachment

The in-situ measurements of work function of a cathode in the argon gas tungsten arc during operation at atmospheric pressure were carried out simultaneously with measurements of surface temperature of the cathode [7]. This technique was based on the photoelectric effect at the surface of the tungsten cathode with the use of a pulse laser system. The effective work functions of pure W, W-2% ThO_2 and W-2% La_2O_3 electrodes during operation at a current of 200 A were 4.6 eV, 2.8 eV and 3.0 eV from the in-situ measurements. These results were very close to the work functions of W, ThO_2 and La_2O_3

as pure materials obtained from the literature [8]. Therefore, it was concluded that the effective work function of tungsten electrodes adding an emitter material, namely, ThO_2 or La_2O_3, was dominated by the work function of the emitter material even though its addition to the electrode was only 2% in weight. From our previous study [7], we have our image of current attachment at thermionic cathode, as follows. (a) Emitter material plays a role of thermionic emission of electrons due to its lower work function independently of its conditions, namely, solid or liquid. (b) Tungsten weakly contributes to thermionic emission of electrons due to its higher work function. (c) Emitter material below its melting point is scattered on the surface of tungsten, as shown in **Fig. 2**. A size of an emitter material is around 5 μm [1]. The emitter material practically covers about 5% of the tungsten surface because 2 wt% of ThO_2 and La_2O_3 becomes 4 to 6 vol% of ThO_2 and La_2O_3. (d) Emitter material above its melting point covers the whole surface of tungsten. In order to evaluate the current attachment, the space-charge sheath at the cathode surface has to be regularly calculated with thermionic emission of electrons [9, 10]. However, our unified model does not take the sheath into account. Therefore, for simplification, we assume that the role of thermionic emission of electrons by emitter material is replaced with the electrical conductivity of arc plasma on the cathode surface, as shown in **Fig. 3**. If surface temperature of the cathode is higher than the melting point of the emitter material, the electrical conductivity of the arc plasma on the cathode surface is assumed to be a regular value independently of temperature because the emitter material covers the whole surface of tungsten. If surface temperature of the cathode is o the contrary lower than the melting point of the emitter material, the electrical conductivity of arc plasma in one mesh neighboring on the cathode surface is assumed to be 5% of the regular value because the emitter material practically covers about 5% of the tungsten surface. The flux of arc current from one mesh to another mesh is roughly represented by $I = S(\sigma E)$, where S is the area between two meshes. We assume to replace 5%S by 5%σ.

Three types of tungsten electrode, namely, W-2% ThO_2, W-2% La_2O_3 and W-2% CeO_2 are calculated in this paper. The numerical values given to a unified model are tabulated in **Table 1**. These values are from the literature [8]. In the manufacturing process of a tungsten electrode, CeO_2 is reduced to Ce_2O_3 after sintering in pure hydrogen atmosphere [11], and then we also assume that the whole CeO_2 of W-2% CeO_2 electrode is changed to Ce_2O_3 in this paper.

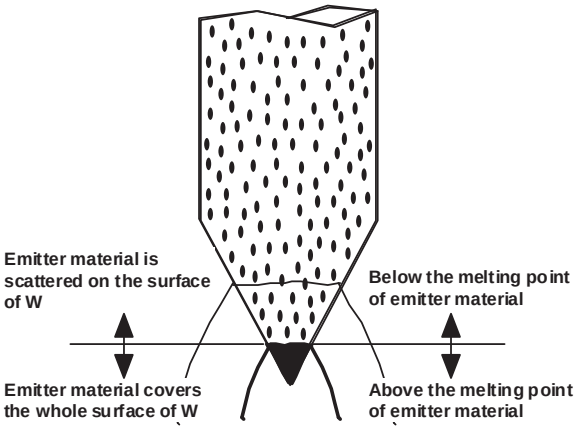

Fig. 2 An image of current attachment.

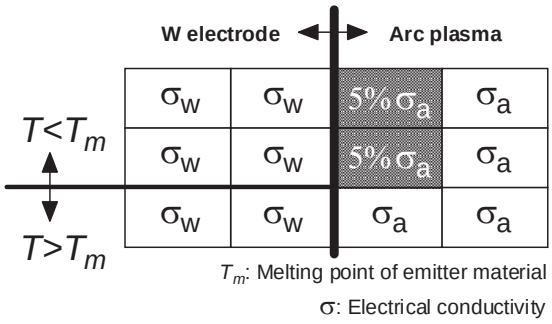

Fig. 3 Treatment of current attachment for a unified arc electrode model.

Table. 1 Numerical values given to a unified model.

Emitter	ϕ (eV)	M.P. (K)	A (A/cm^2K^2)
W	4.5	3653	70.0
ThO_2	2.7	3323	5.0
La_2O_3	3.1	2490	96.0
Ce_2O_3*	3.2 (CeO_2: 3.2)	1963 (CeO_2: 2873)	30.0 Arbitrary value

*CeO_2 is reduced to Ce_2O_3 after sintering in H2 atmosphere.

4. Results and discussion

Figure 4 shows two-dimensional temperatures and fluid flow velocities of gas tungsten arcs for various kinds of electrodes at 200 A of arc current and 5 mm of arc length. These calculations were made for the steady state. The difference between calculated arc voltages for various electrodes is negligible and the value of the arc voltage is about 11.2 V. This tendency was pointed out by experiments [1]. However, the plasma state of the arc column is locally affected by the electrode types. Specifically, the maximum temperature of arc plasma close to the cathode tip for W-2% ThO_2 reaches 19,000 K and it is the highest value in comparison with the other temperatures for W-2% La_2O_3 and W-2% CeO_2, because the current attachment at the cathode tip is constricted by a centralized limitation of liquid area of ThO_2 due to its higher melting point. This higher temperature of the plasma close to the cathode tip at the arc axis would play an important role in the production of a hard arc flame. In cases of W-2% La_2O_3 and W-2% CeO_2, the liquid areas of La_2O_3 and Ce_2O_3 are widely expanded at the cathode tip due to their lower melting points and then produce uniform current attachments at the cathode, resulting a soft arc flame.

Figure 5 shows temperature distributions at electrode surfaces. The maximum temperatures at the tip are 3776 K, 3620 K and 3210 K for W-2% ThO_2, W-2% CeO_2 and W-2% La_2O_3, respectively. These are good agreement with experimental results reported by Haidar and Farmer [12]. The tip temperature of W-2% La_2O_3 during operation is clearly lower than that of W-2% CeO_2 although both work functions of La_2O_3 and Ce_2O_3 are almost the same as shown in **Table 1**. This reason is deduced from a difference of the Richardson constant between 96.0 A/cm^2K^2 in La_2O_3 and 30.0 A/cm^2K^2 in Ce_2O_3. **Figure 6** shows arc pressure distributions at the anode surface. The maximum arc pressure for W-2% CeO_2 reaches 395 Pa and then it is similar to 391 Pa for W-2% La_2O_3. However, the maximum arc pressure for W-2% ThO_2 is clearly lower than these. Sadek measured arc pressure distributions at a water-cooled copper anode by a semiconductor transducer, as shown in **Fig. 7** [1]. Since he, unfortunately, employed 45 degree for the conical tip angle of tungsten electrode and 3 mm for the arc length, we can not compare both results of experiment and calculation directly. However, his experimental results show that the maximum arc pressures of W-2% CeO_2 and W-2% La_2O_3 are almost the same but that for W-2% ThO_2 is clearly lower than these. This tendency is very similar to the tendency given by calculations as shown in **Fig. 6**, although the absolute values of arc pressure in both cases are different due to differences of a few conditions as stated above. **Figure 8** shows current density distributions at 0 mm of axial distance in **Fig. 1**. The maximum current density for W-2% ThO_2 is the highest in comparison with those for W-2% La_2O_3 and W-2% CeO_2. However, the current density for W-2% ThO_2 drastically decreases toward the radius and then it is lower than those for W-2% La_2O_3 and W-2% CeO_2 at around 0.5 mm to 2 mm in the radius. This characteristic of current density distribution for W-2% ThO_2 locally leads to the highest values in the tip temperature of the cathode, in the temperature of the arc plasma and in the fluid flow velocity of the cathode jet, but it produces the lowest value of the arc pressure at the anode surface because an average momentum of the cathode jet for W-2% ThO_2 is smaller than those for the other two electrodes due to more uniform current density distributions for W-2% La_2O_3 and W-2% CeO_2 than that for W-2% ThO_2, as shown in **Fig. 8**. From the above results, it can be concluded that the current attachment at thermionic cathode for gas tungsten arc at atmospheric pressure is dependent on work function, melting point and the Richardson constant of emitter materials.

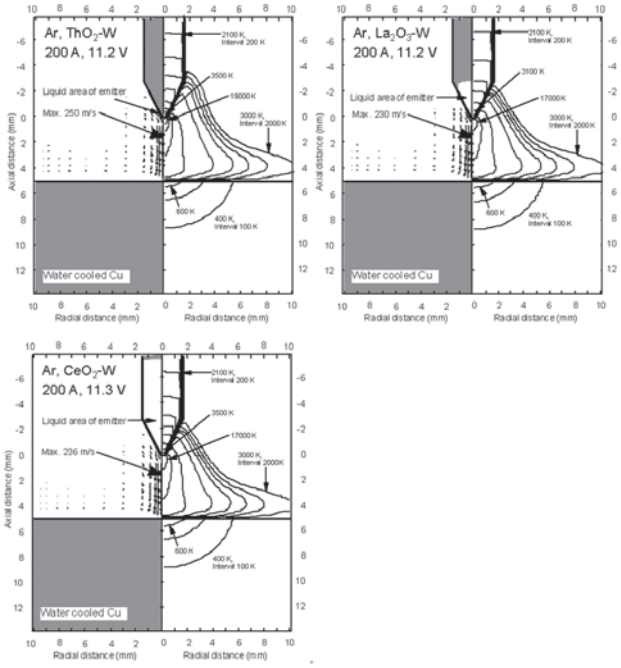

Fig. 4 Temperatures and fluid flow velocities of gas tungsten arcs for various types of electrode.

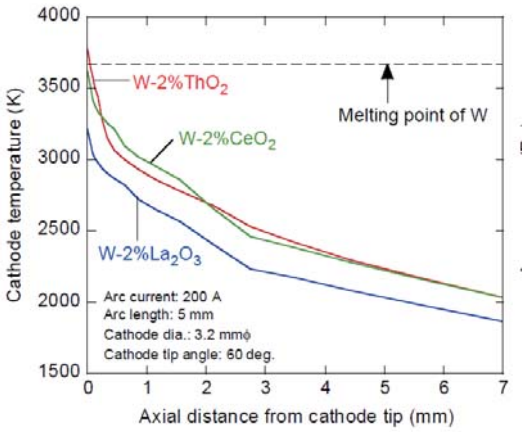

Fig. 5 Temperatures of electrode surface.

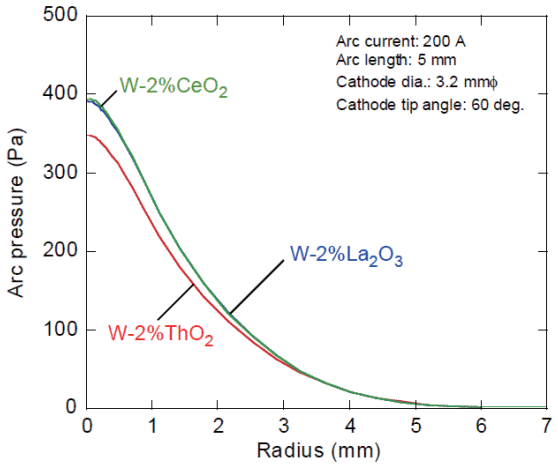

Fig. 6 Arc pressures at anode surface.

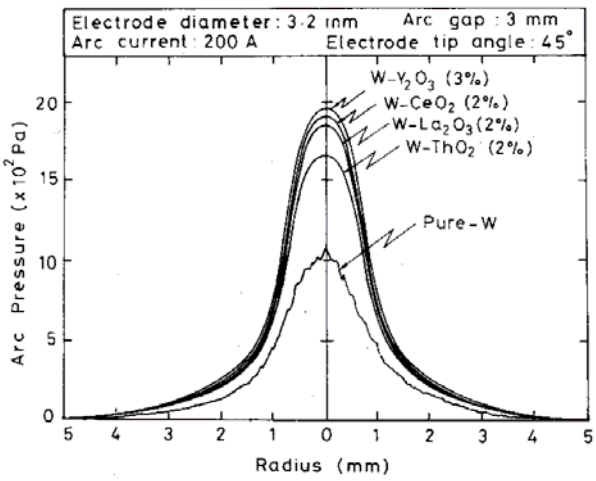

Fig. 7 Experimental results of arc pressure at anode surface [1].

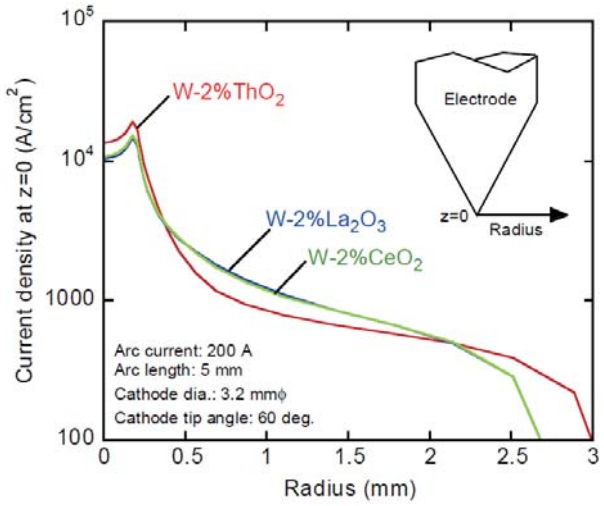

Fig. 8 Current density distributions at the tip of tungsten electrode.

4. Conclusions

The conclusions of this study are summarized as follows.

(1) Study of the current attachment at the thermionic cathode for a gas tungsten arc at atmospheric pressure was examined from numerical calculations of an arc-electrode unified model.
(2) It is suggested that the current attachment at the thermionic cathode was dependent on work function, melting point and the Richardson constant of emitter materials.
(3) The maximum temperature of arc plasma close to the cathode tip for W-2% ThO_2 reached 19,000 K and it was the highest value in comparison with the other temperatures for W-2% La_2O_3 and W-2% CeO_2, because the current attachment at the cathode tip was constricted by a centralized limitation of liquid area of ThO_2 due to its higher melting point. This higher temperature of plasma close to the cathode tip at the arc axis would play an important role in production of a hard arc flame.
(4) In the cases of W-2% La_2O_3 and W-2% CeO_2, the liquid areas of La_2O_3 and Ce_2O_3 were widely expanded at the cathode tip due to their lower melting points and which then produce uniform current attachments at the cathode, resulting a soft arc flame.
(5) The tip temperature of W-2% La_2O_3 during operation was clearly lower than that of W-2% CeO_2 although both work functions of La_2O_3 and Ce_2O_3 were almost the same. This reason was deduced from a difference of the Richardson constant between 96.0 A/cm^2K^2 in La_2O_3 and 30.0 A/cm^2K^2 in Ce_2O_3.

References

1) Sadek AA, Ushio M and Matsuda M; Metall. Trans. A, 1990; 21 A: p3221-3236.
2) Tanaka M et. al.; Plasma Chem. & Plasma Process., 2003; 23: p585-606.
3) Mita T; private communication, 2006.
4) Tanaka M, Ushio M and Lowke JJ; JSME Int. J., Series B, 2005; 48: p.397-404.
5) Lowke JJ and Tanaka M; J. Phys. D: Appl. Phys., 2006; 39: p.3634-3643.
6) Patanker SV; Numerical Heat Transfer and Fluid Flow, Hemisphere Publishing Corporation, 1980.
7) Tanaka M et. al.; J. Phys. D: Appl. Phys., 2005; 38: p.29-35.
8) Fomenko VS: Emission Properties of Materials, Kiev, Naukova Dumka, 1970.
9) Morrow RR and Lowke JJ; J. Phys. D: Appl. Phys., 1993; 26: pp.634-642.
10) Ushio M et. al.; J. Phys. D: Appl. Phys., 1994; 27: p.561-566.
11) Ushio M et.al.; Plasma Chem. & Plasma Process., 1991; 11: p.81-101.
12) Haidar J and Farmer AJD; J. Phys. D: Appl. Phys., 1995; 28: p.2089-2094.